

# MANUFACTURING AND MEASUREMENTS OF MILLIMETER WAVE LENSES IN SUBSTRATE INTEGRATED WAVEGUIDE

---



Universidad  
Politécnica  
de Cartagena



ECIT

The Institute of Electronics,  
Communications and  
Information Technology

2010  
**NEWfocus**  
2015

*New frontiers in mm/sub-mm waves  
integrated dielectric focusing systems  
June 2010 - June 2015*

**ESF Activity:** New Frontiers in Millimetre / Sub-Millimetre Waves Integrated Dielectric Focusing Systems (NewFocus)

**Date of visit (starting date):** 04/08/2013

**Duration:** 1 week

**Project title:** Manufacturing and Measurements of Millimeter Wave Lenses in Substrate Integrated Waveguide

**Reference Number:** 5716

---

#### **Exchange Scientist**

Alejandro Javier Martínez Ros  
Universidad Politécnica de Cartagena  
Antiguo Cuartel de Antigones  
Plaza del Hospital, 1  
30202 Cartagena, Spain  
Email: [alejandro.martinez@upct.es](mailto:alejandro.martinez@upct.es)

#### **Host Institution**

Queen's University of Belfast  
Northern Ireland Science Park  
Queen's Road Queen's Island  
Belfast BT3 9DT, UK

## Summary

1. Purpose of the visit
2. Description of the work carried out during the visit
3. Description of the main results obtained
4. Future collaboration with host institution (if applicable)

## 1. Purpose of the visit

The main objective of this short time stay has been to use the manufacturing and measurements facilities of QuB ECIT's laboratories, in order to measure the designed prototypes of a new class of microwave/millimeter-wave lenses in substrate integrated waveguide (SIW) technology, and to perform an experimental campaign.



**Fig. 1 View of the ECIT building in Belfast.**

Particularly, the capability of these novel SIW leaky-wave antennas (LWAs) to radiate broadside in the far-field regime has been experimentally verified. Also these experiments have showed how with a simple device manufactured in a single substrate, with low-profile and easy-feeding, many exciting potential applications in security and medical imaging systems, hyperthermia, wireless sensors, wireless power-transfer systems, non-radiative wireless communication, non-contact high-speed interconnects, or enhanced RFID readers can be performed.

The proposed short time visit of one week of duration has been held from 04/08 to 10/08. During this stay I have performed an experimental campaign to measure the electrical performance of the designed antennas, using ECIT's anechoic chamber. These antennas have been fabricated using photolithographic and milling technologies, and using standard microstrip to SIW transition to feed them.

Particularly, input matching and near- and far-field radiation pattern measurements (including gain) have been needed to validate the promising results obtained with theory. Finally, the ability to increase the directivity of the radiation pattern by properly changing the antenna printed-circuit geometry has also been demonstrated.

These successful experimental results will be combined with theoretical data and the proposed design methodology, to submit a paper to an international journal in the field of Antenna/Microwave Engineering. Also, future work on enhanced designs will be proposed as a result of this collaborative work between UPCT and QuB ECIT.

## 2. Description of the work carried out during the visit

The main tasks carried out during this exchange visit have been the design, manufacturing and measurement of several prototypes of leaky-wave antennas in SIW technology operating at the frequency of 15 GHz. The antennas have been built in a commercial substrate Rogers RT/duroid 5880 by using milling technology. In addition, standard SMA connectors were soldered in order to have an easy feeding of the antennas (see Fig. 2).

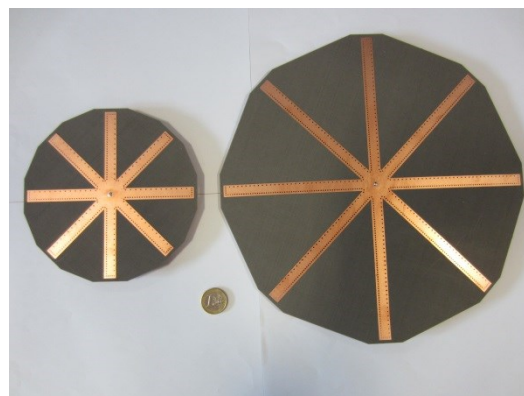


**Fig. 2 Detailed view of the feeding of the LWA: a) Rear view and b) top view.**

During this short term stay two prototypes with different size of the radial array radiating at broadside have been manufactured and measured, with the purpose of demonstrating the capability to tailor the radiation pattern of the antenna while keeping high radiation efficiency. Particularly, the designs manufactured have been the following:

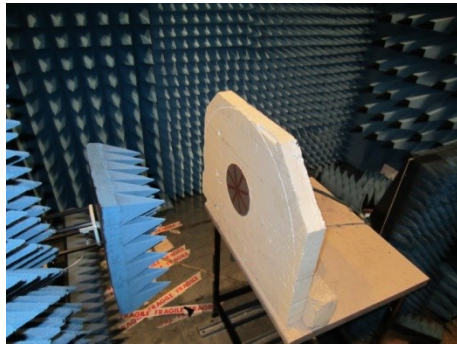
- Radial array radiating at broadside with radius of 3 lambda
- Radial array radiating at broadside with radius of 6 lambda

Fig. 4 shows a picture of the two manufactured prototypes with different lengths in SIW technology.

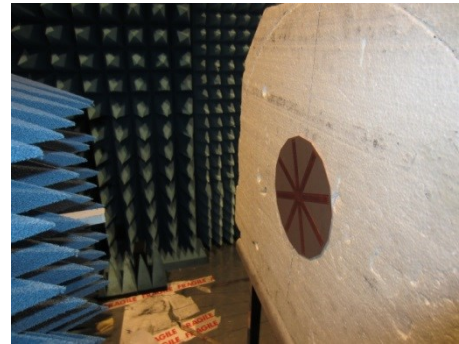


**Fig. 3 Photography of the two prototypes manufactured and measured at the QuB ECIT.**

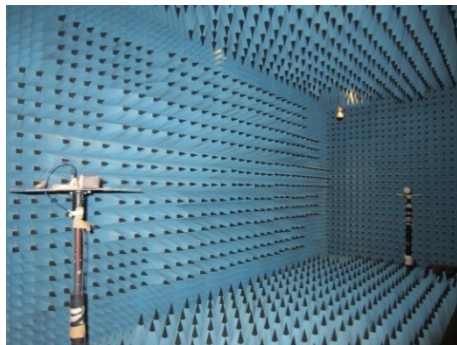
Once the prototypes were manufactured, a measurement campaign was carried out during the final part of the stay, in order to validate the electrical performances of the designed antennas, using ECIT's near- and far-field anechoic chambers (see Fig. 4). Particularly, input matching and radiation pattern measurements have been measured and a good agreement between theoretical and experimental performances has been found, as it will be shown in the next section. In this way, the ability to easily tune the radiation pattern by modifying the antenna printed-circuit dimensions has been demonstrated.



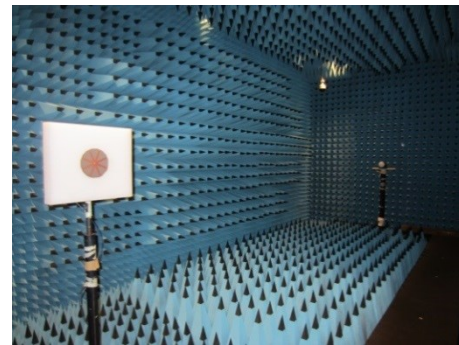
a)



b)



c)



d)

**Fig. 4** Set-up for the measurements inside the anechoic chambers. a) and b) near-field measurements, and c) and d) far-field measurements.

### 3. Description of the main results obtained

In this section the main results obtained as consequence of the work carried out during this exchange visit, are described. The capability to control the radiation performances along the antenna length, is demonstrated with radiation pattern and input matching measurements of both prototypes manufactured.

Fig. 5 shows the input matching simulated and measured for both antennas. It can be seen a good agreement between both results. In particular some slight differences are observed for the case of the larger antenna, but still having a measured  $S_{11}$  below -10dB at the design frequency of 15 GHz.

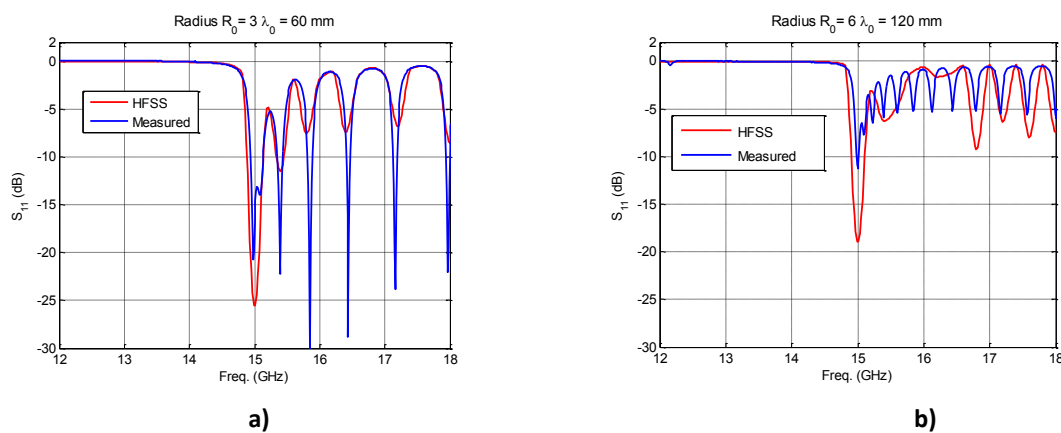


Fig. 5 Input matching measured and simulated for both prototypes: a) Radius  $3\lambda$  and b) radius  $6\lambda$ .

#### – Radiation Patterns

One of the characteristics of this array configuration is that the resulting radiation diagram is linearly polarized, as is illustrated in Fig. 6. For these antennas, measurements both in far- and near-field chambers have been carried out. Due to the versatility of the near-field measurements to select between several polarizations and frequencies, this set-up has been chosen to obtain the results showed in this report. However, the calibration to obtain gain measurements has been performed with the far-field chamber (see Fig. 4c).



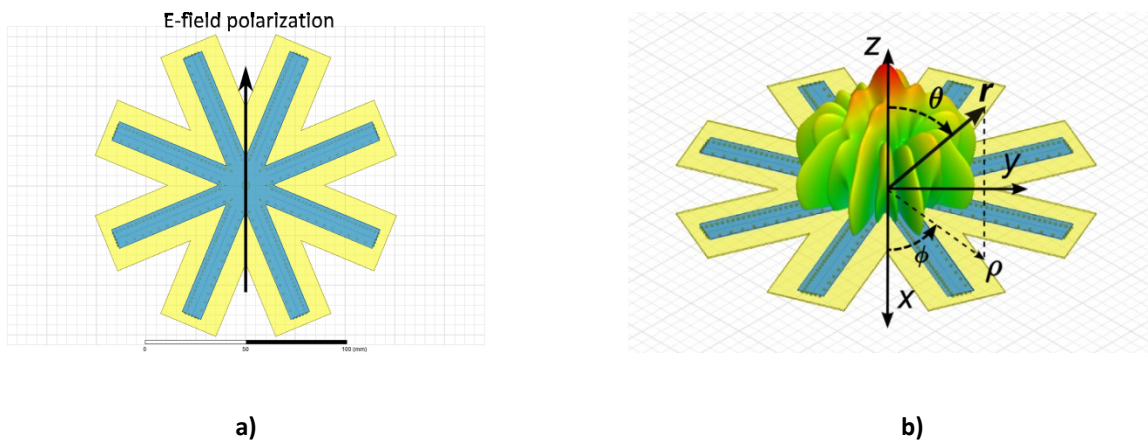


Fig. 6 a) Radiated E-field polarization and b) three dimensional radiation pattern.

### Radius $3\lambda = 60$ mm

Fig. 7a shows the far-field radiation pattern for the H-plane ( $\phi=90$ ) at the design frequency of 15 GHz and for the co-pol component. Measured and simulated results are compared, obtaining good agreement. Moreover, the cross-polarization (X-pol) is represented in Fig. 7b, and levels around -15dB are observed at broadside direction ( $\theta=0$ ).

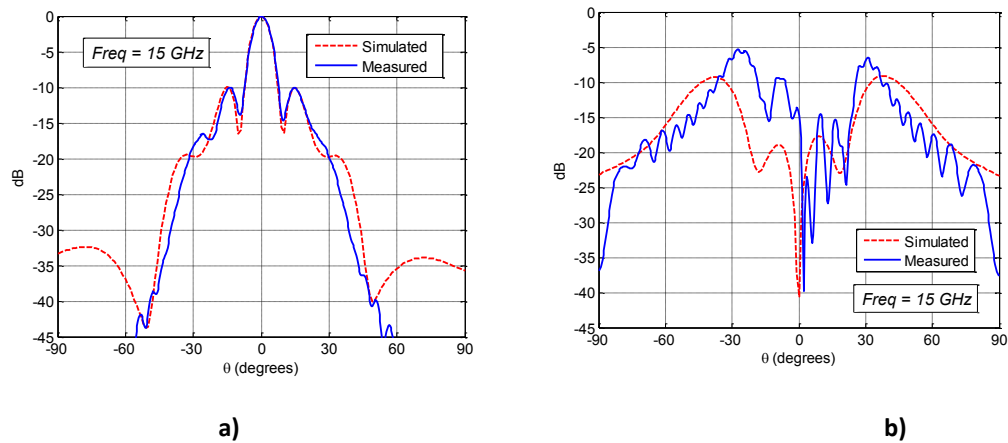


Fig. 7 H-plane radiation pattern ( $\phi=90$ ): a) Co-pol and b) X-pol component.

Measured E-plane ( $\phi=0$ ) is represented in Fig. 8 and compared with simulated results, and good agreement between both results is obtained. Moreover, for this plane is also observed how the X-pol component is -35 dB below the co-pol component.

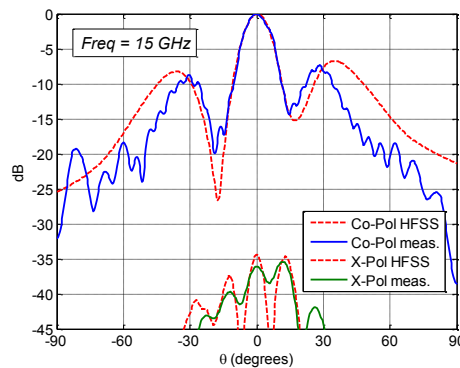


Fig. 8 E-plane radiation pattern ( $\phi=0$ ) co-pol and X-pol components.

### Radius $6\lambda = 120$ mm

Next the radiation patterns of the second prototype, which has a radius of  $6\lambda$ , are shown for different planes. Fig. 9 shows the co-pol component at the H-plane for the design frequency of 15 GHz. Measured results are compared with simulated ones, and good agreement is observed. Moreover, the X-pol component is also represented in Fig. 9b, and a level of -25 dB below the co-pol component is obtained at broadside direction.

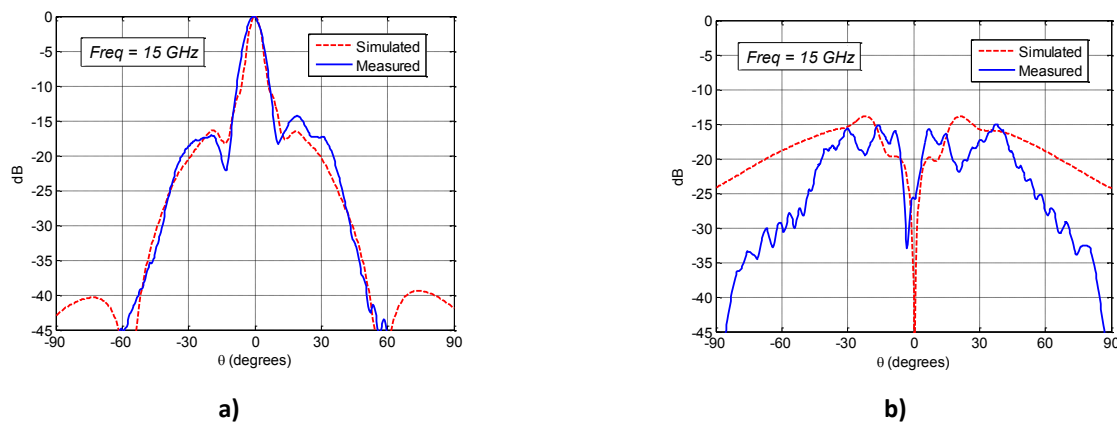


Fig. 9 H-plane radiation pattern ( $\phi=90$ ): a) Co-pol and b) X-pol component.

Finally, the E-plane radiation pattern is also represented in Fig. 10 together with its X-pol component, and compared with simulated results. It can be seen a very good X-pol discrimination around -35 dB. Moreover, some differences between measured and simulated radiation patterns are observed.



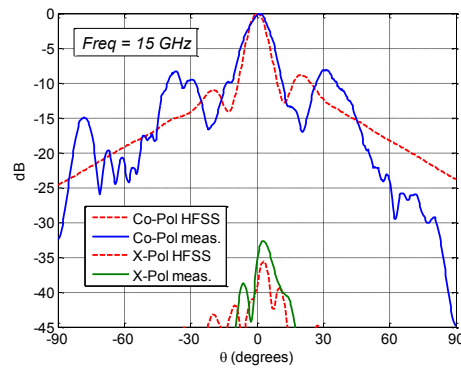


Fig. 10 E-plane radiation pattern ( $\phi=0$ ) co-pol and X-pol components.

#### 4. Future collaboration with host institution (if applicable)

The work developed during this stay, will allow to continue with several common projects between the Universidad Politécnica de Cartagena (UPCT) and Queen's University of Belfast (QuB). Moreover, these successful experimental results will be combined with theoretical data and the proposed design methodology, to submit a paper to an international journal in the field of Antenna Engineering. Also, future work on enhanced designs will be proposed as a result of this collaborative work between UPCT and QUB-ECIT.